KSME Journal, Vol. 2, No. 1, pp. 9~18, 1988.

BOUNDARY LAYER FLOW OVER A FINITE FLAT PLATE WITH A CONSTANT SLIP VELOCITY

Yong Kweon Suh* and Taik Sik Lee**

(Received november 23, 1987)

Two-dimensional incompressible laminar flow induced by a constant slip velocity on the surface of a finite flat plate is studied both analytically and numerically for large Reynolds numbers. It turned out that the thickness of the thin layer downstream of the trailing edge increases in square root of the distance from the trailing edge. Numerical integration of the boundary layer equations for the whole flow field confirmed two asymptotic natures of the flow field; near the trailing edge the analytic result is approached, and far downstream of the plate the jet flow solution is attained.

Key Words: Boundary Layer, Flat Plate, Thin Layer, Jet Flow Theory, Keller's Box Method

1. INTRODUCTION

The problem considered in this paper stems from the need to investigate the structure of the steady streaming flow near the rear stagnation point of a bluff body under high-frequency-oscillations. For instance, when a circular cylinder submerged in a viscous fluid oscillates horizontally in a high frequency, the steady motion of the fluid is induced around the cylinder due to the nonlinear effect of the Navier-Stokes equations (Schlichting, 1955). The accompanying drift of fluid elements may have consequences of practical importance, such as transport of sediment (Batchelor, 1977) around the piles of offshore structures near the sea bottom (the wave instead of the cylinder then induces the steady flow motion, in this case).

The problem is now to solve the flow field with slip velocity on the cylinder surface, zero velocity in the far-field, and suitable conditions for symmetry. In this case when Re is large, where Re is Reynolds number based on the velocity of the streaming flow and the radius of the cylinder, there develop a boundary layer on the surface, thin but thicker than the Stokes layer, and a thin shear layer (jet flow) along the horizontal line extended from the rear stagnation point of the cylinder. The classical boundary layer theory can be applied for this case for the whole flow field except the small region near the rear stagnation point.

Stuart (1966) presented the series solution for this problem, but he stated that the solution seemed unlikely to converge near that point. Duck and Smith (1979), in an attempt to find out the reason for the discrepancy between the theoretical and experimental results for the streaming problem, considered the oscillating cylinder in a large tank. Their series solution was also insufficient to resolve the detailed flow field near that point. They showed a rigorous study concerning the impact of the jet-like boundary layer in the earlier paper (Smith and Duck, 1977), and presented a conjectured flow pattern during the collision of the opposing jets.

Difficulties associated with the analytic approach to this problem are; first, the slip velocity vanishes at the rear stagnation point resulting in the nonlinearity in the governing equations for the local flow field and the complexity in representing the velocity profile at the point, and second, the fluid elements turn sharply through the corner which may even cast doubt about the validity of the double deck structure applied by Smith and Duck (1977).

As a first step to resolve that problem, we simplify the geometry and the boundary conditions to avoid the above difficulties. First, the slip velocity is taken constant throughout the surface, and second, the cylinder is replaced by a flat plate with a finite length. Thus the problem now becomes to solve two-dimensional incompressible laminar flow induced by a constant slip velocity on the surface of a finite flat plate, where the plate is motionless.

According to the general boundary layer theory, it is known that whenever the boundary layer meets an abrupt change in the boundary condition it responds to it through a thin layer near the surface of the body; see (Straford, 1954) and (Curle, 1981) for the change in the pressure gradient, (Goldstein, 1930) for the change in the surface condition, and (Suh, 1986) for a corner problem. Goldstein (1930) studied the uniform flow past a finite flat plate, and showed that the thickness of the thin layer developed downstream of the trailing edge increases like $O(x_1^{1/3})$ and that the governing equation for this region is non-linear, where x_1 is measured from the trailing edge along the streamwise direction. In his solution, however, the normal component of velocity becomes infinite at $x_1=0^+$. This singularity actually became the basis for the foundation of the triple deck theory (Smith, 1982). The lower deck, which corresponds to the thin region of $O(x_1^{1/3})$ for small x_1, is governed by the non-linear equation. This non-linearity comes from the fact that the velocity on the surface is zero up to the trailing edge at which the streamwise velocity increases abruptly, and thus the convective terms of the boundary layer equations are balanced by the diffusive

*Department of Mechanical Engineering, Dong-A University, Pusan 604-714, Korea
**Department of Mechanical Engineering, Seoul National University, Seoul 151-742, Korea

term and are no longer linearized. In the present problem, however, there exists a finite amount of velocity on the surface, and hence the governing equations are expected to be of linear form, since the solution of the leading order equation for the thin layer is conjectured to be the slip velocity itself as is also shown in this paper. Consequently the thickness of the thin layer may be different in power of x_1 from that of the Goldstein's problem.

On the other hand, intitutively it is expected that the flow mechanism far downstream would resemble that of the well known jet flow problem (Schlichting, 1955).

The purpose of this study is to investigate the boundary layer equations subject to a sudden change in a boundary condition in the restriction that the whole flow field is induced by the slip velocity on the surface. The numerical method is also used to support the analysis. Section 2 deals with the formulation of the problem and finds the similarity solution for the upstream region $x_1>0$. Section 3 is concerned with the analytic solution near the trailing edge, whereas section 4 is for the region far downstream. Section 5 shows the numerical solutions of the boundary layer equations for the whole region.

2. FORMULATION OF THE PROBLEM

We consider two-dimensional laminar flow of an incompressible fluid at high Reynolds numbers over a flat plate with a finite length. The flow otherwise undisturbed is induced by a constant slip velocity U_o on the plate occupying the space $o \le x^* \le l$ as shown in Fig. 1. Then on the assumption that a boundary layer exists, the appropriate governing equations for determining a steady motion in the boundary layer are

$$\frac{\partial u}{\partial x}+\frac{\partial v}{\partial y}=0 \tag{1}$$

$$u\frac{\partial u}{\partial x}+v\frac{\partial u}{\partial y}=-\frac{dp}{dx}+\frac{1}{Re}\frac{\partial^2 u}{\partial y^2} \tag{2}$$

where x, y, u, v, and p are non-dimensional variables based on $2l$, U_o, and ρ the density of the fluid. Re is the Reynolds number defined as $\frac{2U_o l}{\nu}$ in which ν is the kinematic viscosity. The reason for $2l$ instead of l lies only on the algebraic simplicity. The pressure gradient term $\frac{dp}{dx}$ in (2) can be ignored to the unknown order of $\frac{1}{Re}$, because $u \to o$ as $y \to \infty$

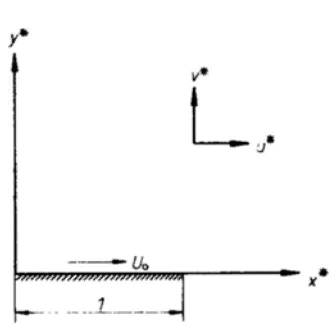

Fig. 1 Definition of the problem in the physical coordinates

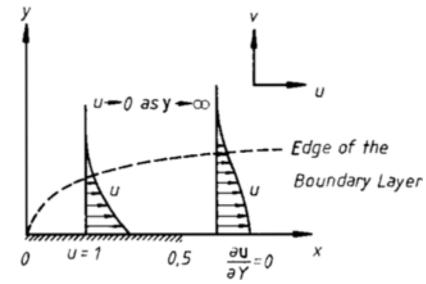

Fig. 2 The coordinate system and the boundary conditions in dimensionless quantities

asymptotically. Further, we stretch variables v and y as

$$v=\frac{1}{\sqrt{Re}}V, \quad y=\frac{1}{\sqrt{Re}}Y$$

upon which (1) and (2) become

$$\frac{\partial u}{\partial x}+\frac{\partial V}{\partial Y}=0 \tag{3}$$

$$u\frac{\partial u}{\partial x}+V\frac{\partial u}{\partial Y}=\frac{\partial^2 u}{\partial Y^2} \tag{4}$$

The boundary conditions are

$$V=0 \quad \text{on } Y=0 \text{ for all } x>0 \tag{5}$$

$$u=1 \quad \text{on } Y=0 \text{ for } 0<x\le\frac{1}{2} \tag{6}$$

$$\frac{\partial u}{\partial Y}=0 \quad \text{on } Y=0 \text{ for } \frac{1}{2}<x \tag{7}$$

$$u\to 0 \quad \text{as } Y\to\infty \tag{8}$$

The third condition (7) is based on the fact that the flow field for $\frac{1}{2}<x$ be symmetric about $Y=0$. Fig. 2 shows the geometry concerned and the boundary conditions in non-dimensional variables.

We now introduce the similarity variable z as used in the classical boundary layer flow problem for the flat plate:

$$z=\frac{Y}{\sqrt{2x}} \tag{9}$$

Then we put

$$u=f'(x,\ z) \tag{10}$$

so that

$$\Psi=\sqrt{2x}\,f(x,\ z), \tag{11}$$

$$V=-\frac{\partial \Psi}{\partial x}=-\frac{1}{\sqrt{2x}}(f-zf')-\sqrt{2x}\,f_x \tag{12}$$

where $\Psi=Re\psi$ is the stretched stream function from ψ, and

$$u=\frac{\partial \Psi}{\partial Y}=\frac{\partial \psi}{\partial y}, \quad V=-\frac{\partial \Psi}{\partial x}, \quad v=-\frac{\partial \psi}{\partial x}. \tag{13}$$

Prime denotes differentiation with respect to z and the subscript x to x. Substituting (10), (12) and their derivatives into (4), we obtain

$$f''' + ff'' = 2x(f'f'_x - f''f_x) \tag{14}$$

The boundary conditions (5) to (8) then reduce to

$$f(x,\ 0) = 0 \tag{15}$$

$$f'(x,\ 0) = 1 \text{ for } 0 < x \leq \frac{1}{2} \tag{16}$$

$$f''(x,\ 0) = 0 \text{ for } \frac{1}{2} < x \tag{17}$$

$$f'(x,\ z) \to 0 \text{ as } z \to \infty \tag{18}$$

If the plate were semi-infinite, the whole flow field would be represented by the similarity solution with one variable z, i. e., the terms on the right-hand side of (14) would vanish. The present case, however, is for a finite plate, and thus it is clear that the similarity solution satisfying all the boundary conditions of (15) to (18) does not exist. Nevertheless, we may assume that the similarity solution is an exact solution up to the trailing edge for (14) with (15), (16), and (18). The reason is that, as far as the governing equations are concerned, they are of parabolic type and hence the upstream influence of the flow field due to the transition in the boundary condition from (16) to (17) is impossible. A very similar situation arises for the Goldstein's problem (Goldstein, 1930) in which the Blasius solution applies to the region between the leading edge and the trailing edge of the finite flat plate (Van Dyke, 1975).

Thus, let $f_s(z)$ be the similarity solution of $f(x, z)$ valid for $0 < x \leq \frac{1}{2}$, then

$$f_s''' + f_s f_s'' = 0, \tag{19}$$
$$f_s(0) = 0, \tag{20}$$
$$f'_s(0) = 1, \tag{21}$$
$$f'_s(z) \to 0 \text{ as } z \to \infty \tag{22}$$

Solution of (19) satisfying (20) to (22) starts from z ;

$$f_s(z) = \sum_{k=1}^{\infty} b_k z^k \tag{23}$$

$$b_1 = 1,\ b_2 = \lambda = \frac{f''_s(0)}{2},$$

$$b_k = \frac{-1}{k(k-1)(k-2)} \sum_{i=1}^{k-2} (k-i-1)(k-i-2) b_i b_{k-i-1},$$
$$(k \geq 3)$$

where $\lambda = -0.31380768\cdots$ from the numerical integration. The following is then obtained :

$$u_0 = u(\tfrac{1}{2},\ Y) = \Big[f'_s(z)\Big]_{x=\frac{1}{2}} = f'_s(Y)$$
$$= 1 + 2\lambda Y - \frac{1}{3}\lambda Y^3 - \frac{1}{6}\lambda^2 Y^4 + \frac{1}{20}\lambda Y^5 + \frac{11}{180}\lambda^2 Y^6 + \cdots \tag{24}$$

$$\Big[V(x,\ Y)\Big]_{Y\to\infty} = -\frac{1}{\sqrt{2x}}\Big[f_s - zf'_s\Big]_{z\to\infty} = \frac{-1.14274}{\sqrt{2x}} \tag{25}$$

3. ASYMPTOTIC SOLUTION NEAR THE TRAILING EDGE

The solution presented in the preceding section is valid only up to $x = \frac{1}{2}$ just downstream of which the boundary condition changes abruptly from (16) to (17). A typical situation can be found near the trailing of a finite flat plate subject to a uniform flow. It is generally noticed that whenever a sudden change takes place in the boundary condition or in the pressure gradient the boundary layer responds to it through a thin viscous layer. For the flow downstream of the trailing edge of a flat plate subject to a uniform flow, this thin layer turned out to grow like $o(x_1^{1/3})$ where $x_1 = x - 1$ is measured from the trailing edge(Goldstein, 1930). For the present problem the exponent of x_1 for the thin layer thickness is anticipated to be different from 1/3 because the velocity for $Y \to o$ remains $O(1)$. We let this exponent $\frac{1}{m}$ unknown a priori. We put

$$\eta = \frac{Y}{\xi},\quad \xi = (mx_1)^{\frac{1}{m}} \tag{26}$$

and

$$\Psi = \xi^{m-1} F(\xi,\ \eta) \tag{27}$$

so that

$$u = \xi^{m-2} F'(\xi,\ \eta), \tag{28}$$

$$V = -\frac{1}{\xi}\Big\{(m-1)F + \xi F_\xi - \eta F'\Big\} \tag{29}$$

Substituting (28), (29) and their derivatives into (4) we get

$$F''' + (m-1)FF'' - (m-2)F'F' = \xi(F'F'_\xi - F''F_\xi) \tag{30}$$

The leading order equation of (30) for small ξ will take the same form on the left-hand side and 0 on the right-hand side. As $\xi \to 0$, $\eta \to \infty$ for fixed Y, and thus F' should approach 1 asymptotically for this limit. If the third term of (30) were to exist, say $m \neq 2$, either the first term or the second must survive for large η, which due to the intrinsic nature of the equation may not be possible. Thus we must choose $m = 2$. Then (30) simply becomes

$$F''' + FF'' = \xi(F'F'_\xi - F''F_\xi) \tag{31}$$

The boundary condition (5) and (7) are equivalent to

$$F(\xi,\ 0) = F''(\xi,\ 0) = 0 \tag{32}$$

while the condition $u = u_0$ at $x_1 = 0$ requires that

$$\lim_{\eta\to\infty} F'(\xi,\ \eta) = u_0. \tag{33}$$

Now, by (24), the above condition can be written as

$$\lim_{\eta\to\infty} F'(\xi,\ \eta) = 1+\xi(2\lambda\eta)+\xi^3(-\frac{1}{3}\lambda\eta^3) + \xi^4(-\frac{1}{6}\lambda^2\eta^4)+\xi^5(\frac{1}{20}\lambda\eta^5)+\xi^6(\frac{11}{180}\lambda^2\eta^6) + \cdots = \sum_{k=0}^{\infty}\xi^k(a_k\eta^k) \quad (34)$$

Thus the appropriate expansion for $F(\xi,\ \eta)$ must be

$$F(\xi,\ \eta) = F_0(\eta)+\xi F_1(\eta)+\xi^2F_2(\eta)+\cdots \quad (35)$$

so that

$$F_0'''+F_0F_0''=0$$
$$F_1'''+F_0F_1''-F_0'F_1'+2F_0''F_1=0$$
$$F_2'''+F_0F_2''-2F_0'F_2'+3F_0''F_2=F_1'F_1'-2F_1F_1''$$
$$\cdots\cdots$$
$$F_n'''+F_0F_n''-nF_0'F_n'+(n+1)F_0''F_n=\sum_{k=1}^{n-1}\left\{kF_k'F'_{n-k}-(k+1)F_kF''_{n-k}\right\}$$
$$\cdots\cdots \quad (36)$$

The boundary conditions are

$$F_n(0)=F_n''(0)=0, \quad (37)$$
$$\lim_{\eta\to\infty}F_n'(\eta)=a_n\eta^n$$

First, the non-linear equation for F_0 and the corresponding boundary conditions are satisfied only with

$$F_0=\eta \quad (38)$$

All the other equations are linear and with F_0 known take the form as follows;

$$F_n'''+\eta F_n''-nF_n'=G_n(\eta), \quad (39)$$

where $G_n(\eta)$ is the known function;

$$G_n(\eta)=\sum_{k=1}^{n-1}\left\{kF_k'F'_{n-k}-(k+1)F_kF''_{n-k}\right\} \quad (40)$$

Thus, the complete solution $F_n(\eta)$ will be sum of the complementary solution $F_{nh}(\eta)$ and the particular solution $F_{np}(\eta)$. The complementary solution $F_{nh}(\eta)$ satisfying the boundary conditions at $\eta=0$ must start from η. It is found that

$$F'_{nh}(\eta)=C_nM(-\frac{n}{2},\ \frac{1}{2},\ \frac{-\eta^2}{2}) \quad (41)$$

where $M(a,\ b,\ \zeta)$ is the confluent hypergeometric function(Abramowitz & Stegun, 1972), and

$$M(a,\ b,\ \zeta)=1+\frac{a}{b}\zeta+\frac{(a)_2}{(b)_2}\frac{\zeta^2}{2!}+\frac{(a)_3}{(b)_3}\frac{\zeta^3}{3!}+\cdots$$

in which

$$(a)_n=\frac{\Gamma(a+n)}{\Gamma(a)}$$

is the Pochhammer's symbol. Thus for small η,

$$F'_{nh}(\eta)=C_n\left\{1+n\frac{\eta^2}{2!}+n(n-2)\frac{\eta^4}{4!} + n(n-2)(n-4)\frac{\eta^6}{6!}+\cdots\right\}. \quad (42)$$

The asymptotic expansion for large η is

$$F'_{nh}(\eta)\backsim C_n\frac{\Gamma(\frac{1}{2})}{\Gamma(\frac{n+1}{2})}\sum_{k=1}^{KL}\frac{(n+2k-2)!}{(n-2)!k!2^{n/2+k}}\eta^{n-2k}, \quad (43)$$

where k_L is integer of $\frac{n}{2}$. Generally for large η the asymptotic expansion for $F_n(\eta)$ must have descending series starting from η^{n+1}. Putting the multiplying constant β with double subscript, $F_n(\eta)$ will be

$$F_n(\eta)\backsim\sum_{k=1}^{n+2}\beta_{n,\ n-k+2}\ \eta^{n-k+2} \quad (44)$$

Then (40) can be written for large η as

$$G_n(\eta)\backsim\sum_{m=0}^{n}w_m\eta^m \quad (45)$$

where

$$w_m=\sum_{k=1}^{n-1}\{-(k+1)d^m+ke^m\} \quad (46)$$
$$d_m=\sum_{i+j=n+2-m}\beta_{k,k-i+2}\beta_{l,l-j+2}(l-j+2)(l-j+1),$$
$$(i,\ j\geq1,\ i\leq k+2,\ j\leq l)$$
$$e_m=\sum_{i+j=n-2-m}\beta_{k,k-i+2}\beta_{l,l-j+2}(k-i+2)(l-j+1),$$
$$(i,\ j\geq0,\ i\leq k+1,\ j\leq l+1)$$

and $l=n-k$. It turned out that $\beta_{m,m}$ vanishes in obtaining the solutions up to $F_4(\eta)$. In the following, we shall prove that this is true for all $F_n(\eta)$. First we prove that $w_n=w_{n-1}=0$. With $m=n$, (46) becomes

$$w_n=\sum_{k=1}^{n-1}(k+1)(n-k+1)(2k-n)\beta_{k,k+1}\beta_{n-k,n-k+1}.$$

Replacing k by $n-k$ results in

$$w_n=\sum_{n\ k=1}^{n-1}(n-k+1)(k+1)(n-2k)\beta_{n-k,n-k+1}\beta_{k,k+1}$$

and thus, for even $(n-1)$ all therms are cancelled out by each other, and for odd$(n-1)$ one remaining term when $k=\frac{n}{2}$ also vanishes because $(n-2k)=0$. Now it is clearly seen that when $m=n-1$ either $\beta_{k,k-i+2}$ or $\beta_{l,l-j+2}$ becomes zero because $\beta_{k,k}=\beta_{l,l}=0$ which means that $w_{n-1}=0$. And thus $G_n(\eta)$ does not contain η^n and η^{n-1}. Next we assume that the particular solution $F'_{np}(\eta)$ for large η starts from η^{n-2}, i. e.,

$$F'_{np}(\eta)\backsim\sum_{i=0}^{n-2}h_i\eta^i \quad (47)$$

upon which and (45), (39) becomes

$$\sum_{m=0}^{n-4}(m+2)(m+1)h_{m+2}+\sum_{m=0}^{n-2}(m-n)h_m=\sum_{m=0}^{n-2}w_m.$$

Therefore

$$h_{n-2}=-\frac{1}{2}w_{n-2}$$
$$h_{n-3}=-\frac{1}{3}w_{n-3}$$
$$h_m=\frac{1}{m-n}\{w_m-(m+2)(m+1)h_{m+2}\},$$
$$(m=n-4,\ n-5,\cdots,\ 0).$$

Consequently it is proved that the assumption (47) is correct and accordingly $\beta_{m,m}=0$. Thus for large η,

$$F_n(\eta)\backsim\sum_{m=0}^{n+1}\beta_{n,m}\eta^m \tag{48}$$
$$\beta_{n,m}=\frac{h_{m-1}}{m}+s_m$$
$$s_m=\begin{cases} C_n\dfrac{\Gamma\left(\frac{1}{2}\right)}{\Gamma\left(\frac{n+1}{2}\right)}\dfrac{(n+2k-2)\,!}{(n-2)\,!k\,!(n-2k+1)2^{n/2+k}}\ ;\ \text{if } n+1-m \text{ is even}\\ 0\ ;\ \text{else}\end{cases}$$

where $n-2k+1=m$, and $h_{m-1}=0$ if $m=n+1$ and $m=n$.
On the other hand we assume that for small η

$$F'_{np}=\sum_{k=0}^{\infty}b_k\eta^k \tag{49}$$

$$G_n=\sum_{k=0}^{\infty}r_k\eta^k \tag{50}$$

Then by substituting (49) and (50) into (39), and collecting coefficients in like powers of η, we get

$$b_{k+2}=\frac{1}{(k+2)(k+1)}r_k+\frac{(n-k)}{(k+2)(k+1)}b_k \tag{51}$$

It is clear that the second term on the right-hand side of (51) generates nothing more than the complementary solution if either $b_0\neq0$ or $b_1\neq0$. Hence

$$b_0=b_1=0$$

is a compulsory condition to obtain a purely particular solution; i.e., F'_{np} starts from η^2 for small η. C_n is then obtained from the condition at infinity by

$$C_n=\frac{\Gamma\left(\frac{n+1}{2}\right)}{\Gamma\left(\frac{1}{2}\right)}2^{\frac{n}{2}}a_n \tag{52}$$

Using an explicit expression, we write u for large η as follows;

$$\begin{aligned} u&=F_0'+\xi F_1'+\xi^2F_2'+\xi^3F_3'+\xi^4F_4'+\cdots\\ &=a_0+\xi(2\beta_{1,2}\eta)+\xi^2(2\beta_{2,3}\eta^2+\beta_{2,1})\\ &\quad+\xi^3(4\beta_{3,4}\eta^3+2\beta_{3,2}\eta+\eta_{3,1})+\cdots\\ &=(a_0+2\beta_{1,2}Y+3\beta_{2,3}Y^2+4\beta_{3,4}Y^3+\cdots)\\ &\quad+\xi(\qquad 0 \qquad)\\ &\quad+\xi^2(\beta_{2,1}+2\beta_{3,2}Y+3\beta_{4,3}Y^2+4\beta_{5,4}Y^3+\cdots)\\ &\quad+\xi^3(\beta_{3,1}+2\beta_{4,2}Y+3\beta_{5,3}Y^2+4\beta_{6,4}Y^3+\cdots)\\ &\quad+\cdots \end{aligned} \tag{53}$$

Thus for fixed small ξ, the expansion (35) is not adequate in describing the flow field for large Y.

For large Y, the asymptotic expansion (53) suggests us to expand u as

$$u=f_0'(Y)+\xi f_1'(Y)+\xi^2f_2'(Y)+\cdots \tag{54}$$

so that

$$\Psi=f_0(Y)+\xi f_1(Y)+\xi^2f_2(Y)+\cdots \tag{55}$$

It is clear that $f_0=f_s(Y)$. Substituting these and their derivatives into (4), we obtain the sequence of first order equations as follows

$$\left.\begin{aligned} &f_0'f_1'-f_0''f_1=0\\ &2(f_0'f_2'-f_0''f_2)=f_0'''+f_1''f_1-f_1'f_1'\\ &3(f_0'f_3'-f_0''f_3)=f_1'''+2(f_1''f_2-f_1'f_2')\\ &\quad+(f_2''f_1'-f_2'f_1')\cdots\cdots\\ &n(f_0'f_n'-f_0''f_n)=f'''_{n-2}+\sum_{k=1}^{n-1}(f_k''f_{n-k}\\ &\quad-f_k'f'_{n-k})\cdots\cdots \end{aligned}\right\} \tag{56}$$

The boundary condition is from matching with (5) for small Y, i.e.,

$$\lim_{Y\to0}f'_n(Y)=\beta_{n,1} \tag{57}$$

Solutions of the first 7 terms are obtained:

$$\left.\begin{aligned} f_1&=0\\ f_2&=\frac{1}{2}\left\{(\alpha_2-Y)f_0'+f_0\right\}\\ f_3&=\frac{1}{3}\alpha_3f_0'\\ f_4&=\frac{1}{8}\left\{(\alpha_2-Y)^2f_0''+(Y+\alpha_4)f_0'-f_0\right\}\\ f_5&=\frac{1}{6}\alpha_3(\alpha_2-Y)f_0''+\alpha_5f_0'\\ f_6&=\frac{1}{48}(\alpha_2-Y)^3f_0'''+\left\{\frac{1}{16}(\alpha_2-Y)(2Y+\alpha_4-\alpha_2)\right.\\ &\quad\left.+\frac{1}{18}\alpha_3^2\right\}f_0''+\left(-\frac{1}{16}Y+\alpha_6\right)f_0'+\frac{1}{16}f_0\\ f_7&=\frac{1}{24}\alpha_3(\alpha_2-Y)^2f_0'''+\left\{\left(-\frac{1}{2}\alpha_5+\frac{1}{8}\alpha_3\right)Y\right.\\ &\quad\left.+\frac{1}{2}\alpha_2\alpha_5+\frac{1}{24}\alpha_3\alpha_4-\frac{1}{12}\alpha_2\alpha_3\right\}f_0''+\alpha_7f_0' \end{aligned}\right\} \tag{58}$$

where

$$\alpha_2=\frac{2\beta_{2,1}}{a_1}$$
$$\alpha_3=\frac{3\beta_{3,1}}{a_1}$$
$$\alpha_4=\frac{8\beta_{4,1}}{a_1}+2\alpha_2$$
$$\alpha_5=\frac{\beta_{5,1}}{a_1}+\frac{1}{6}\alpha_3$$
$$\alpha_6=\frac{1}{a_1}(\beta_{6,1}-\frac{1}{8}\alpha_2^3\alpha_3)-\frac{1}{16}(3\alpha_2-\alpha_4)$$
$$\alpha_7=\frac{1}{a_1}(\beta_{7,1}-\frac{1}{4}\alpha_3^2\alpha_2^2)+\frac{1}{2}\alpha_5-\frac{1}{8}\alpha_3$$

The center-line velocity defined as $u_c=u(x,o)$ is then obtained from (42) and (52);

Table 1 Asymptotic nature of u and V obtained by the analytic method for the boundary layer equations for small x_1

x_1	u	V
$x_1=0$	$f_s'(Y)$	$-f_s(Y)+Yf_s'(Y)$
$x_1>0$	$1+\frac{2\sqrt{2}}{\Gamma\left(\frac{1}{2}\right)}\lambda\sqrt{2x_1}\,F_1'(\eta)$ $+\cdots$ for small η	$-(2F_1-\eta F_1')-\sqrt{2x_1}(3F_2-\eta F_2')+\cdots$ for small η
	$f_s'(Y)+x_1(2\lambda^2-Y)f_s''(Y)+\cdots$ for large Y	$-[f_s(Y)-(Y-2\lambda)f_s'(Y)]+\cdots$ for large Y

$$u_c=\sum_{k=0}^{\infty}\frac{\Gamma\left(\frac{k+1}{2}\right)}{\Gamma\left(\frac{1}{2}\right)}2^{k/2}a_k\xi^k \tag{59}$$

Table 1 shows the asymptotic nature of u and V for small x_1.

4. SOLUTION FOR THE REGION FAR DOWNSTREAM ; JET FLOW THEORY

The only driving condition which generates the fluid motion is the inhomogeneous boundary condition at $y=0$, i.e., (6). The induced motion of the fluid is then free of that condition after the trailing edge of the plate, and thus the flow mechanism far downstream will approach to that of the jet flow. Schlichting obtained an exact solution for the two-dimensional laminar jet flow based on the boundary layer equation (Schlichting, 1955):

$$\Psi=2\alpha x_1^{1/3}\tanh\left(\frac{\alpha Y}{3x_1^{2/3}}\right) \tag{60}$$

$$u=\frac{2}{3}\alpha^2 x_1^{-\frac{1}{3}}\left\{1-\tanh^2\left(\frac{\alpha Y}{3x_1^{2/3}}\right)\right\} \tag{61}$$

where

$$\alpha=\left(\frac{9}{8}J_0\right)^{1/3}$$

$$J_0=\int_0^{\infty}u^2dY$$

Integrating (2) with respect to y from 0 to infinity and applying the conditions (5). (7), and (8), we obtain

$$\frac{\partial}{\partial x}\int_0^{\infty}u^2dY=0 \tag{62}$$

which states that J_0 is independent of x, and so x_1. At $x_1=0$,

$$J_0=\int_0^{\infty}u^2dY=\int_0^{\infty}(f_s')^2dY=-f_s''(0)=0.627615 \tag{63}$$

where the third equality comes from (19). Then

$$\alpha=0.89046 \tag{64}$$

5. NUMERICAL SOLUTION OF THE BOUNDARY LAYER EQUATION

Finite difference technique is used to obtain the solution of the boundary layer equation with the aid of a computer. The equation to be solved is (14) and the boundary conditions are (15) to (18). The mesh system is as shown in Fig. 3. The method is based on the so called Keller's box method (Cebeci and Smith, 1974), but the centered difference for the x-derivatives was not successful due to the discontinuity in the boundary condition at $Y=0$ and $x_1=0$. thus we shall use the backward difference for that. Another feature special to the present problem is that the boundary condition at infinity (finite but large in the computational domain) is homegeneous, so that the algorithm of Thomas cannot be directly applied. We write

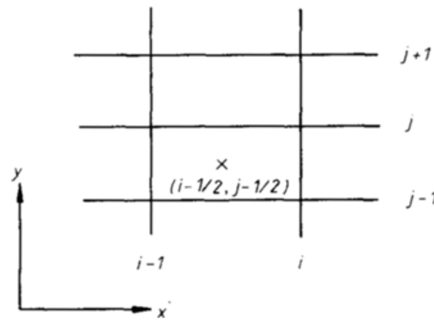

Fig. 3 The mesh system used in the difference formula of the boundary layer equations

$$f(x,\ z)=z-g(x,\ z) \tag{65}$$

Then, the boundary conditions for $g(x,\ z)$ become

$$g(x,\ 0)=0 \tag{66}$$

$$g'(x,\ 0)=0 \quad \text{for } 0<x\leq\frac{1}{2} \tag{67}$$

$$g''(x,\ 0)=0 \quad \text{for } \frac{1}{2}<x \tag{68}$$

$$g'(x,\ z)\to 1 \quad \text{as } z\to\infty \tag{69}$$

so that the condition at infinity is now inhomogeneous. Substituting (65) into (14) and introducing $h(z)$ yield

$$g'=h \tag{70}$$

$$h''-gh'+zh'=2x(h_x+g_xh'-h_xh) \tag{71}$$

The non-linear terms in (71) are linearized by putting for a function ϕ (g or h)

$$\phi=\hat{\phi}+(\phi-\hat{\phi})$$

where $\hat{\phi}$ stands for the old value of ϕ, and by neglecting terms in multiples of $(\phi-\hat{\phi})$ which are assumed to be small. Derivatives in x are resolved by using the backward difference. It results in

$$h''+ph'+qh+rg=s \tag{72}$$

where

$$p = z - \hat{g} - 2x\,\hat{g}_x$$
$$q = 2x\ \{\hat{h}_x + \frac{1}{\Delta x}(\hat{h} - 1)\}$$
$$r = -\left(1 + \frac{2x}{\Delta x}\right)\hat{h}'$$
$$s = \frac{2x}{\Delta x}(\hat{h}^2 - \hat{g}\hat{h}' - h_{i-1}) - \hat{g}\hat{h}'$$

Using the centered difference for the z-derivatives, (67) becomes

$$A_j h_{j-1} + B_j h_j + C_j h_{j+1} + D_j g_j = E_j \tag{73}$$

where

$$A_j = 1 - \frac{p}{2}\Delta z$$
$$B_j = -2 + q\Delta z^2$$
$$C_j = 1 + \frac{p}{2}\Delta z$$
$$D_j = r$$
$$E_j = s$$

Now we apply centered difference to (70) at the mesh point $(i - \frac{1}{2},\ j - \frac{1}{2})$ marked "X" in Fig. 3;

$$g_j = g_{j-1} + \frac{\Delta z}{2}(h_j + h_{j-1}) \tag{74}$$

Using Thomas algorithm, equation (73) can be expressed as

$$h_j = R_j + S_j h_{j-1} + T_j g_{j-1} \tag{75}$$

Substituting (75) into (73) to eliminate h_{j+1} and using (74) to eliminate g_j yields

$$h_j = \frac{E_j - C_j R_{j+1}}{V_j} - \frac{A_j + \frac{\Delta z}{2}(C_j T_{j+1} + D_j)}{V_j} h_{j-1} - \frac{C_j T_{j+1} + D_j}{V_j} g_{j-1} \tag{76}$$

where

$$V_j = B_j + C_j S_{j+1} + \frac{\Delta z}{2}(C_j T_{j+1} + D_j).$$

By comparing (76) with (75), we obtain

$$R_j = \frac{E_j - C_j R_{j+1}}{V_j}$$
$$S_j = -\frac{A_j + \frac{\Delta z}{2}(C_j T_{j+1} + D_j)}{V_j} \tag{77}$$
$$T_j = -\frac{C_j T_{j+1} + D_j}{V_j}.$$

The boundary conditions given by (66) to (69) are

$$g_1 = 0, \tag{78}$$

$$h_1 = \begin{cases} 0, & \text{for } 0 < x \leq \frac{1}{2} \\ \dfrac{R_3 + (S_3 + \frac{\Delta z}{2}T_3)R_2 - 4R_2}{4S_2 - \{S_2(S_3 + \frac{\Delta z}{2}T_3) + \frac{\Delta z}{2}T_3\} - 3} & \text{for } \frac{1}{2} < x \end{cases} \tag{79}$$

$$h_J = 1, \tag{80}$$

where J denotes the end of j. The condition (80) corresponding to (68) is obtained by representing the function $h(z)$ near $z=0$ with a polinomial composed of h_1, h_2, and h_3.

The computational procedure is as follows:

(1) Assume the initial value of $\hat{g}$, $\hat{g}_x$, $\hat{h}$, and $\hat{h}_x$. At $x=0$ $\hat{h}$ is chosen by

$$h = \begin{cases} z & \text{for } 0 < z \leq 1 \\ 1 & \text{for } 1 \leq z \leq z_e \end{cases}$$

where z_e is the upper edge of the domain. At all the other stations of x, the extrapolation from the two previous steps is used to estimate the initial values.

(2) K_j, B_j, $\cdots$, E_j are calculated.

(3) Starting from $j = J-1$, R_j, S_j, and T_j are obtained by (77) up to $j=1$ with $R_J = 1$ and $S_J = T_J = 0$.

(4) Then g_j and h_j are obtained from $j=2$ to $j=J$ using (74) and (75) with g_1 and h_1 given by (78) and (79) or (80) depending on x.

(5) The procedures (2) to (4) are repeated until $|\phi - \hat{\phi}|$ becomes small enough.

(6) x is increased and the procedure (1) to (5) is repeated.

6. RESULTS AND DISCUSSIONS

Table 2 and Fig. 4 show the center-line velocity u_c obtained by the numerical treatment of the boundary layer equations in comparison with that obtained by the analytic method, i.e. (59), and that obtained by the jet flow theory (61). In Table 2, analytic results are for the first 17 terms of equation (32). x used in the numerics #1 of Table 2 is 0.001 for $0.50 \leq x < 0.504$, 0.002 for $0.504 \leq x < 0.520$, 0.005 for $0.520 \leq x < 0.550$, 0.010 for $0.550 \leq x < 0.600$, and 0.020 for $0.600 \leq x$, while that in the numerics #2 is 0.01 for $0.50 \leq x < 0.54$, 0.02 for $0.54 \leq x < 0.60$, 0.04 for $0.60 \leq x < 0.68$, 0.08 for $0.68 \leq x < 0.92$, 0.16 for $0.92 \leq x <$

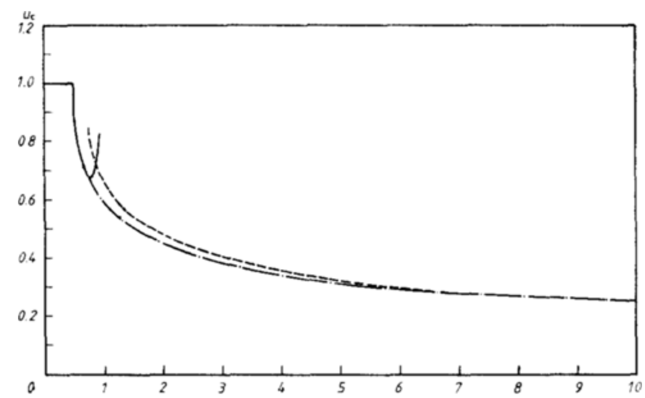

Fig. 4 Center-line velocity u_c; —·—, Numerics; ——, Analytic result (up to 17 terms of Eq. (32)); -----, Jet flow theory

Table 2 Centerline velocity u_c obtained by the analytic method, the numerics, and the jet flow theory

x	Analytic method	Numerics #1	Numerics #2	Jet flow theory
0.51		0.930155	0.936560	
0.52	0.901078	0.900991	0.905756	
0.54	0.861692	0.861315	0.864122	
0.56	0.832424	0.831733	0.834764	
0.59	0.808474	0.807570	0.810408	
0.60	0.787959	0.786781	0.789470	
0.62	0.769904	0.768919		
0.64	0.753728	0.752827	0.755975	
0.66	0.739063	0.738184		
0.68	0.725764	0.724749	0.728093	
0.70	0.713436	0.712342		
0.72	0.702335	0.700819		
0.74	0.692489	0.690065		
0.76	0.684197	0.679989	0.685708	0.828285
0.78	0.678008	0.670513		
0.80	0.674815	0.661572		
0.84		0.645091	0.651869	0.757379
0.92		0.616633	0.623916	0.705867
1.08		0.572192	0.582396	0.633865
1.24		0.538420	0.549910	0.584425
1.56		0.489234	0.505056	0.518447
1.88		0.454216	0.471652	0.474803
2.52		0.406085	0.428232	0.418173
3.00		0.380659		0.389487
3.80		0.349331	0.379119	0.355060
5.08		0.315031	0.346395	0.318311
6.36		0.291163	0.322495	0.293207
7.64		0.273197	0.303988	0.274520
8.00		0.268883		0.270055
8.92		0.258976	0.289067	0.259838

Table 3 Distributions of u obtained by the numerics in comparison with those by the jet flow theory for two stations of $x=3.0$, and 8.0.

z	at $x=3.0$		at $x=8.0$	
	Numerics #1	Jet flow theory	Numerics #1	Jet flow theory
0.00	0.380659	0.389487	0.268882	0.270055
0.21	0.378310	0.386823	0.267782	0.268915
0.42	0.371377	0.378976	0.264516	0.265532
0.60	0.362034	0.368434	0.260072	0.260931
0.90	0.340422	0.344194	0.249591	0.250094
1.20	0.312954	0.313690	0.235840	0.235906
1.50	0.281791	0.279511	0.219599	0.219190
2.10	0.216474	0.209453	0.182941	0.181648
3.00	0.131492	0.121979	0.128055	0.125980
4.20	0.060105	0.052680	0.071368	0.069347
5.40	0.025648	0.021334	0.036849	0.035486
7.20	0.006726	0.005262	0.012559	0.012181

1.24, 0.32 for $1.24 \le x < 1.88$, 0.64 for $1.88 \le x < 2.52$, and 1.28 for $2.52 \le x$. It is noted that the analytic result is very close to the numerical solution for x smaller than 0.80 at which the difference is about 2%. On the other hand, the jet flow theory yields better results as x is increased. At $x=3$, u_c obtained by the jet flow theory differs from that of the numerics by 2%, while that at $x=8$ by 0.4% as is also seen in Table 3.

Figure 5 shows distributions of the streamwise velocities obtained by numerics. Noteworthy is that the velocity profile changes abruptly near $x=0.5$, and for small Y. Shown in Fig. 6 (a) and (b) are stream-lines. it is observed that the fluid particles are entrained for $x<0.5$, and detrained for $x>0.5$ for moderate and small Y. The value of Y at $x=0.5$ at which the normal velocity component V changes its direction is

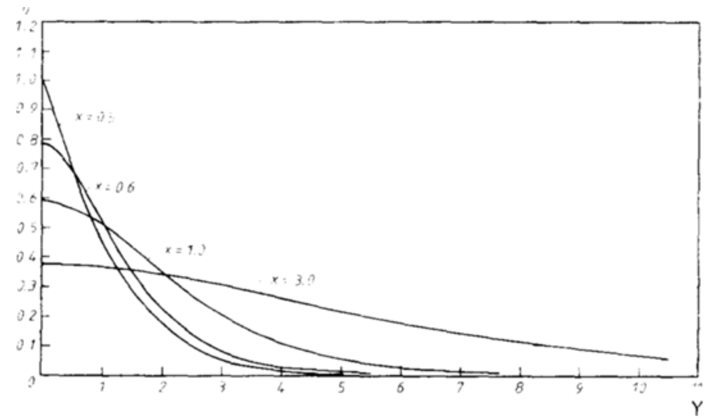

Fig. 5 Distributions of u obtained by the numerics for four stations of $x=0.5$, 0.6, 1.0, and 3.0

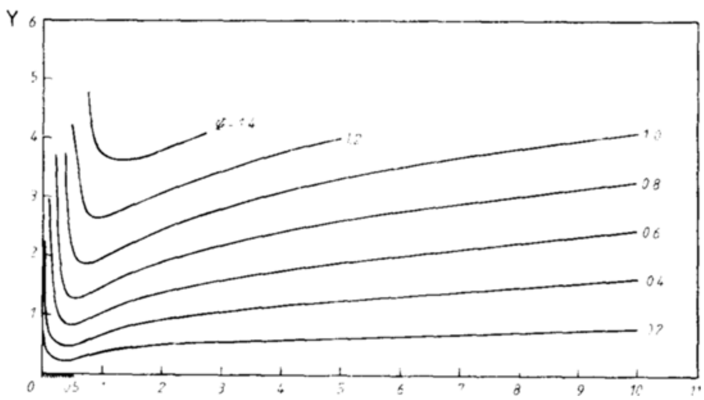

(a) Overall view

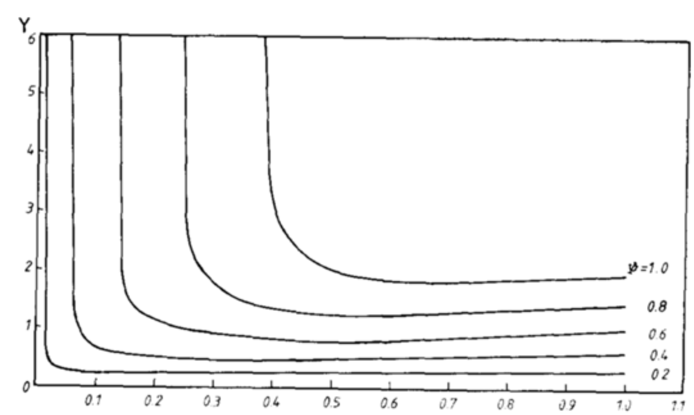

(b) Enlarged view near the plate.

Fig. 6 Streamline patterns

found to be 1.040 as is calculated by the asymptotic equation shown in Table 1.

The analytic solution obtained in section 4 is studied concerning its convergence. As is shown in Fig. 7 and Fig. 8, the series (59) seems to diverge for all x_1, but it gives more accurate result for smaller x_1. It implies that an optimum number of terms which gives the most accurate result depending on x_1 exists; for u_c, average of which is found to be 0. 64385 being 0.2% off from that of the numerics 0.64509 (Fig 8 (a)), while at $x_1=0.50$, $k=2\sim 11$ gives the average u_c of 0.5910

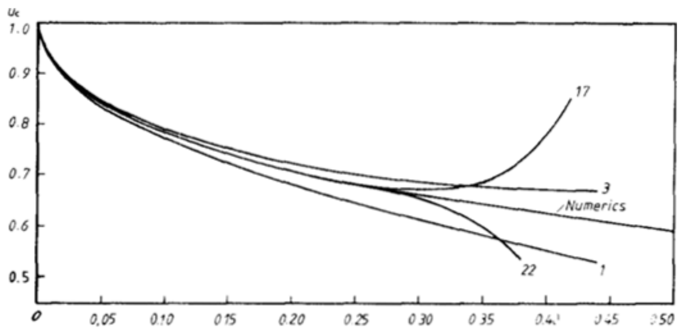

Fig. 7 Center-line velocity u_c obtained by the analytic method. Number of terms included in evaluating (32) are shown in the end of each curve

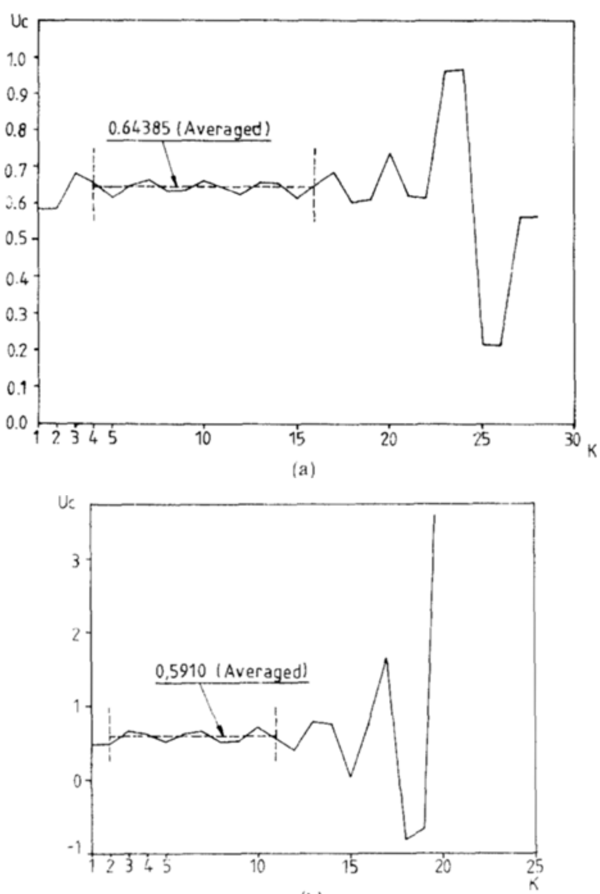

Fig. 8 Nature of the asymptotic series (32). The first K terms are used to evaluate u_c at (a) $x_1=0.34$, and (b) $x_1=0.5$

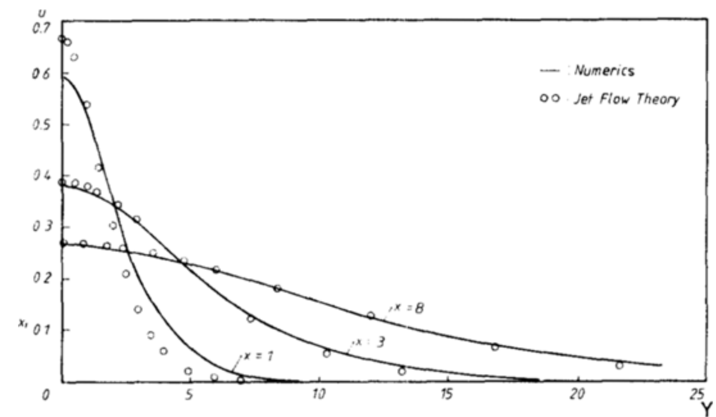

Fig. 9 Distributions of u obtained by the numerics in comparison with those by the jet flow theory for three stations of $x=1.0$, 3.0, and 8.0

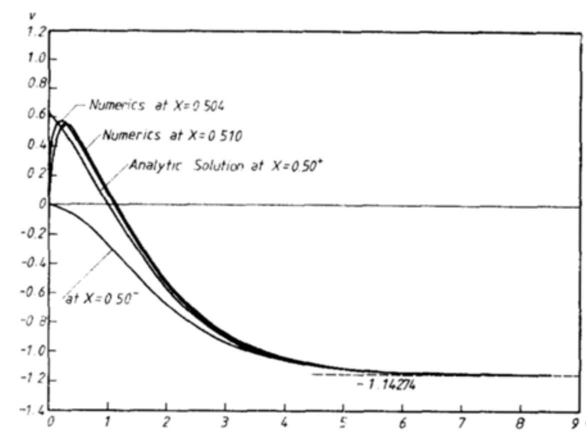

Fig. 10 Distributions of V obtained by the numerics and the analytic method for the region very close to the trailing edge

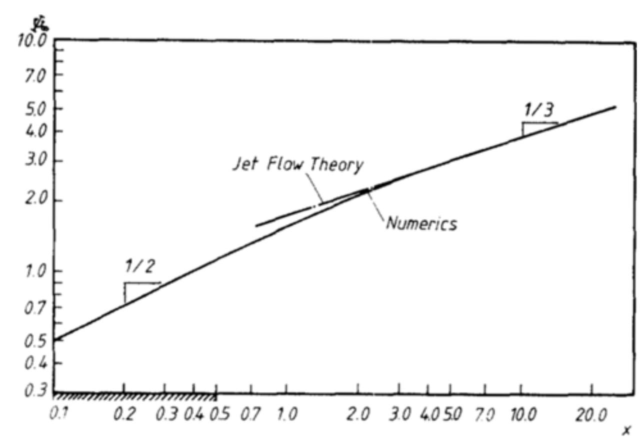

Fig. 11 Asymptotic nature of the numerical result for Ψ_∞ of the present problem for large x

being 0.3% off from that of the numerics 0.59272 (Fig. 8(b)).

Figure 9 compares distributions of u obtained by the numerics with those by the jet flow theory at three stations of x. It is clearly seen that the two results agree better as x is increased.

Figure 10 shows the distribution of V for small x_1. As is found by the analytic solution (Table 1), V shifts abruptly at $x=0.5$ in the region within the boundary layer which is also confirmed by the numerics as shown in Fig. 10. This abrupt shift in V occurrs only at moderate Y. Because of this discontinuity in V, we may need to construct a smaller region near the trailing edge within which the new scheme like the triple deck (Smith, 1982) can be devised to resolve the singularity. It may be similar to the two deck scheme used by Smith & Duck (1977) and by Merkin & Smith (1982) whose problems are concerned with the natural convection so that the streamwise velocity component vanishes far from the wall; the present problem is hence similar to them in this sense but differs in that the present one contains the finite amount of velocity at the wall.

Figure 11 shows Ψ_∞ defined as $\Psi_\infty = \Psi_{Y\to\infty}$ versus x in log-log scales. Ψ_∞ for the numerical result is evaluated at the upper edge of the computational domain. It is seen that the power $\frac{1}{3}$ of equation (60) is attained for large x.

REFERENCES

Abramowitz, M. and Stegun, I.A., 1972, "Handbook of Mathematical Functions", Dover Pub., Inc., New York, pp. 504~510.

Batchelor, G.K., 1977, "An Intruduction to Fluid Dynamics", Camb. Univ. press, p. 363.

Cebeci, T. and Smith. A.M.O., 1974, "Analysis of Turbulent Boundary Layers", Academic Press, pp. 265~269.

Curle, N., 1981, "Development and Separation of a Laminar Boundary Layer with an Exponentially Increasing Pressure Gradient", Q. J. Mech. Appl. Math., Vol. 34, pp. 383~395.

Duck, P. W. and Smith, F. T., 1979, "Steady Streaming Induced Between Oscillating Cylinders", J. Fluid Mech., Vol. 91, pp. 93~110.

Goldstein, S., 1930, "Concerning Some Solutions of the Boundary Layers Equations in Hydrodynamics", Proc. Camb. Phil. Soc., Vol. 26, pp. 1~30.

Merkin, J.H. and Smith, F.T., 1982, "Free Convection Boundary Layers near Corners and Sharp Trailing Edges", ZAMP, Vol. 33, pp. 36~52.

Schlichting, H., 1955, "Boundary-Layer Theory", Seventh Ed., McGraw-Hill Inc., pp. 179~183.

Smith, F.T., 1982, "On the High Reynolds Number Theory of Laminar Flows", IMA J. Appl. Math., Vol. 28, pp. 207~281.

Smith, F. T. and Duck, P. W., 1977, "Separation of Jets or Thermal Boundary Layers from a Wall", Q. J. Mech. Appl. Math., Vol. 30, Pt. 2, pp. 143~156.

Stratford, B.S., 1954, "Flow in the Laminar Boundary Layer near Separation", ARC R. & M. 3002.

Stuart, J. T., 1966, "Double Boundary Layers in Oscillatory Viscous Flow", J. Fluid Mech., Vol. 24, pp. 673~687.

Suh, Y. K., 1986, "On Laminar Viscous Flow in a Corner", Ph. D. Dissertation, State Univ. of New York at Buffalo, Buffalo, N. Y., U.S.A.

Van Dyke, M., 1975, "Perturbation Methods in Fluid Mechanics", The Parabolic Press, Stanford, California, pp. 121~147.